

Role of histone deacetylase inhibitor-induced reactive oxygen species and DNA damage in LAQ-824/fludarabine antileukemic interactions

Roberto R. Rosato,¹ Jorge A. Almenara,¹
Sonia C. Maggio,¹ Stefanie Coe,¹ Peter Atadja,³
Paul Dent,² and Steven Grant^{1,2}

Departments of ¹Medicine and ²Biochemistry, Massey Cancer Center, Virginia Commonwealth University, Richmond, Virginia and ³Department of Oncology, Novartis Institutes for Biomedical Research, East Hanover, New Jersey

Abstract

The role of reactive oxygen species (ROS) production on DNA damage and potentiation of fludarabine lethality by the histone deacetylase inhibitor (HDACI) LAQ-824 was investigated in human leukemia cells. Preexposure (24 h) of U937, HL-60, Jurkat, or K562 cells to LAQ-824 (40 nmol/L) followed by fludarabine (0.4 μ mol/L) dramatically potentiated apoptosis ($\geq 75\%$). LAQ-824 triggered an early ROS peak (30 min–3 h), which declined by 6 h, following LAQ-824-induced manganese superoxide dismutase 2 (Mn-SOD2) upregulation. LAQ-824/fludarabine lethality was significantly diminished by either ROS scavengers *N*-acetylcysteine or manganese (III) tetrakis (4-benzoic acid) porphyrin or ectopic Mn-SOD2 expression and conversely increased by Mn-SOD2 antisense knock-down. During this interval, LAQ-824 induced early (4–8 h) increases in γ -H2AX, which persisted (48 h) secondary to LAQ-824-mediated inhibition of DNA repair (e.g., down-regulation of Ku86 and Rad50, increased Ku70 acetylation, diminished Ku70 and Ku86 DNA-binding activity, and down-regulated DNA repair genes *BRCA1*, *CHEK1*, and *RAD51*). Addition of fludarabine further potentiated DNA damage, which was incompatible with cell survival, and triggered multiple proapoptotic signals including activation of nuclear caspase-2 and release of histone H1.2 into the cytoplasm. The latter event induced activation of Bak and culminated in pronounced mitochondrial injury and

apoptosis. These findings provide a mechanistic basis for understanding the role of early HDACI-induced ROS generation and modulation of DNA repair processes in potentiation of nucleoside analogue-mediated DNA damage and lethality in leukemia. Moreover, they show for the first time the link between HDACI-mediated ROS generation and the recently reported DNA damage observed in cells exposed to these agents. [Mol Cancer Ther 2008; 7(10):3285–97]

Introduction

Histone deacetylase inhibitors (HDACI) are currently a major focus of interest as anticancer agents (1, 2). Their mode of action is most likely multifactorial, including disruption of corepressor complexes, induction of oxidative injury, up-regulation of death receptors, generation of lipid second messengers (e.g., ceramide), interference with chaperone protein function, modulation of nuclear factor- κ B activity, etc. (2–4).

Recent studies suggest that HDACIs interact synergistically with cytotoxic agents such as fludarabine in human leukemia cells (5). Fludarabine (2-fluoroadenine 9- β -D-arabinofuranoside-monophosphate) is a purine analogue with significant activity against B-cell malignancies, including chronic lymphocytic leukemia and indolent non-Hodgkin's lymphoma (6). It has also shown activity in combination with other agents in patients with acute myelogenous leukemia (7). 2-Fluoroadenine 9- β -D-arabinofuranoside-monophosphate is rapidly dephosphorylated in the plasma to its nucleotide derivative, F-ara-A, which is transported across cell membranes by a facilitated nucleoside diffusion system (8). It is then rephosphorylated by the salvage pathway enzyme deoxycytidine kinase and ultimately converted to its lethal form, 2-fluoroadenine 9- β -D-arabinofuranosidetriphosphate (9). 2-Fluoroadenine 9- β -D-arabinofuranosidetriphosphate inhibits multiple enzymes involved in DNA synthesis, including DNA polymerase, DNA primase, and ribonucleotide reductase (10), and also disrupts DNA repair (11, 12). 2-Fluoroadenine 9- β -D-arabinofuranoside-monophosphate incorporation into DNA is required for lethality (13). Previous studies revealed that prior exposure of Jurkat lymphoblastic leukemia cells to marginally toxic concentrations of the benzamide HDACI MS-275 (500 nmol/L), an inhibitor of class I HDACs (1, 2), for 24 h sharply increased mitochondrial injury and apoptosis in response to minimally toxic fludarabine concentrations (500 nmol/L), resulting in highly synergistic antileukemic interactions (5). However, although reactive oxygen species (ROS) generation was implicated in this interaction, the mechanism by which such events occurred was not elucidated.

Received 4/22/08; revised 6/10/08; accepted 7/13/08.

Grant support: National Cancer Institute grants CA63753, CA93738, and CA100866 and a V Foundation award.

The costs of publication of this article were defrayed in part by the payment of page charges. This article must therefore be hereby marked *advertisement* in accordance with 18 U.S.C. Section 1734 solely to indicate this fact.

Requests for reprints: Steven Grant, Division of Hematology/Oncology, Massey Cancer Center, Virginia Commonwealth University, MCV Station Box 230, Richmond, VA 23298. Phone: 804-828-5211; Fax: 804-828-8079. E-mail: stgrant@vcu.edu

Copyright © 2008 American Association for Cancer Research.

doi:10.1158/1535-7163.MCT-08-0385

ROS generation has been identified as a mediator of HDACI-induced cell death (3) as well as that triggered by nucleoside analogues (14). However, ROS also act indirectly by modulating signaling pathways (15). The purpose of this study was to investigate mechanisms underlying the role of HDACI-mediated ROS generation in potentiation of fludarabine lethality. The present results indicate that preexposure of human leukemia cells to minimally toxic concentrations of the hydroxamate pan-HDACI LAQ-824 induces early and transient ROS increases that lead to sustained DNA damage, reflected by γ -H2AX and phospho-ATM induction, as well as down-regulation/inactivation of DNA repair proteins, but does not trigger a pronounced apoptotic response. However, subsequent exposure to a minimally toxic fludarabine concentration dramatically increases both γ -H2AX and phospho-ATM expression, but not ROS generation, accompanied by caspase-2 activation, cytosolic translocation of histone 1.2 and Bak activation, and extensive apoptosis. Collectively, these results provide for the first time evidence linking HDACI-induced early ROS generation with induction of marginally lethal DNA damage, which, in conjunction with HDACI-mediated DNA repair disruption, strikingly sensitizes leukemia cells to fludarabine. These findings also support a model in which LAQ-824 and fludarabine cooperate to impair DNA repair and, in so doing, dramatically increase the lethal consequences of HDACI-mediated DNA damage.

Materials and Methods

Cells and Cell Culture

U937, HL-60, K562, and Jurkat human leukemia cells were obtained from the American Type Culture Collection and maintained as described previously (16). Genetically modified U937 cells were prepared by transfection of the corresponding vectors using an Amaxa nucleofector. For manganese superoxide dismutase 2 (Mn-SOD2) transfection, a full-length cDNA was cloned into pcDNA3.1 (Invitrogen) oriented in both directions (sense pcDNA3.1-SOD2 and antisense pcDNA3.1-SOD-AS, respectively). Cells expressing various small interfering RNA (siRNA) were generated using the pSilencer vector (Ambion) and the following oligonucleotides: BAK (5'-GGATTCA-GCTATTCTGGAAGA-3'), histone H1.2 (5'-AAGAGCG-TAGCGGAGTTTGTC-3'), and procaspase-2 sequence 13 (5'-AATGTGGAAGCTCCTCAACTTG) and sequence 18 (5'-AAGCACTGAGGGAGACCAAGC-3'). For controls, pSilencer harboring a scramble oligonucleotide was used (pS-C). All experiments used cells in logarithmic phase (2.5×10^5 /mL).

Drugs and Chemicals

LAQ-824 was provided by Novartis Pharmaceuticals. The pan-caspase inhibitor Boc-D-fmk was purchased from Enzyme System Products. 2-Fluoroadenine 9- β -D-arabino-furanoside-monophosphate was purchased from Sigma-Aldrich. Manganese (III) tetrakis (4-benzoic acid) porphyrin (Mn-TBAP) was purchased from Calbiochem.

Assessment of Apoptosis

Apoptosis was evaluated by Annexin V/propidium iodide (PI; BD PharMingen) staining as described previously (17) and by morphologic assessment of Wright-Giemsa-stained cytospin preparations.

Cell Cycle Analysis

Cell cycle analysis by flow cytometry was done as described previously (18) using a Becton Dickinson FACScan flow cytometer and Verity Winlist software (Verity Software).

Assessment of Mitochondrial Membrane Potential

At the indicated intervals, cells were harvested and 2×10^5 cells incubated with 40 nmol/L DiOC₆ (15 min, 37°C). Mitochondrial membrane potential loss was determined by flow cytometry as described previously (19).

Measurement of ROS Production

Cells were treated with either 20 μ mol/L 2',7'-dichlorodihydrofluorescein diacetate (Molecular Probes) or 5 μ mol/L dihydroethidium (Invitrogen) for 30 min at 37°C. Fluorescence was monitored by flow cytometry and analyzed with CellQuest software as described previously (19).

Analysis of Cytosolic Cytochrome c and Apoptosis-Inducing Factor

A previously described technique was employed to isolate the S-100 (cytosolic) cell fraction (19). For each condition, 30 μ g protein isolated from the S-100 cell fraction was separated and monitored by Western blot.

Determination of Clonogenicity

Pelleted cells were washed extensively and prepared for soft-agar cloning as described previously (5). Cultures were maintained for 10 to 12 days in a 37°C, 5% CO₂ incubator, after which colonies, defined as groups of ≥ 50 cells, were scored.

Western Blot Analysis

Analysis of protein expression by Western blotting was done as described previously (17). In brief, whole-cell pellets were washed and resuspended in PBS and lysed with loading buffer (Invitrogen); 30 μ g total protein for each condition was separated by 4% to 12% Bis-Tris NuPage precast gel system (Invitrogen) and electroblotted to nitrocellulose. After incubation with the corresponding primary and secondary antibodies, blots were developed by enhanced chemiluminescence (New England Nuclear). Primary antibodies for the following proteins were used at the designated dilutions: poly(ADP-ribose) polymerase (1:1,000; BioMol); procaspase-3, cytochrome *c*, and procaspase-9 (1:1,000; BD Transduction Laboratories); caspase-8 (1:2,000; Alexia); Bid (1:1,000; Cell Signaling Technology); actin (1:4,000; Sigma-Aldrich); apoptosis-inducing factor (1:1,000), Mn-SOD2 (1:500), SOD1 (1:4,000), human thioredoxin (1:2,000), and thioredoxin reductase (1:1,000; Santa Cruz Biotechnology); histone H1.2 (1:3,000; Abcam); vitamin D up-regulated protein 1 (VDRP1)/thioredoxin-binding protein 2 (TBP2; MBL; 1:1,000); and γ -H2AX (1:2,000; Upstate/Millipore). Secondary antibodies conjugated to horseradish peroxidase were obtained from Kirkegaard & Perry Laboratories.

Immunofluorescence for Foci Detection

After cytopspin, cells were fixed for 10 min in ethanol/acetic acid (95%/5%) and washed with H₂O, permeabilized 15 min with 0.1% Triton X-100, and washed three times with H₂O and once with PBS. Sections were blocked with PBS/1% bovine serum albumin for 1 h at room temperature and incubated overnight at 4°C in a humidified chamber with appropriate dilutions of mouse monoclonal anti-human phospho-ATM (Ser¹⁹⁸¹) antibody (Cell Signaling Technology). Slides were washed in PBS and incubated (1 h) with FITC anti-mouse antibody (1 mg/mL; Southern Biotech). No positive cells were identified when specific antibodies were replaced by isotype-matched control antibody. Cells were covered using mounting medium for fluorescence with 4',6-diamidino-2-phenylindole (Vector Laboratories).

Comet Assay

The comet assay was done as per the manufacturer's instructions (CometAssay; Trevingen). After treatment, cells were plated on low-melting agarose gel slides and incubated in lysis buffer. Samples were electrophoresed at 25 V, 300 mA for 25 min and, after staining with SYBR Green, analyzed under a fluorescence microscope.

[³H]F-ara-A DNA Incorporation

Incorporation of [³H]fludarabine into DNA was done as described previously (20). The quantity of [³H]F-ara-A incorporated into U937 cell DNA was calculated and expressed as counts/min [³H]F-ara-A/μg DNA.

Extraction of RNA, Reverse Transcription, and RT2 Profiler PCR Array

Total RNA was extracted from U937 cells after treatment using RNeasy isolation Kit (Qiagen). Real-time reverse transcription-PCR analysis of a group of genes involved in DNA damage was done using the DNA damage RT² Profiler PCR array (SuperArray Bioscience) and the SensiMix One-Step kit (Quantace/Bioline) according to the manufacturer's protocol. Gene expression was compared according to the C_T value.

Statistical Analysis

The significance of differences between experimental conditions was determined using either the Student's *t* test for unpaired observations or the ANOVA test for multiple groups. To assess interactions, median dose analysis (21) was used (CalcuSyn; Biosoft). The combination index was calculated for a two-drug combination involving a fixed concentration ratio. Combination index values <1.0 indicate a synergistic interaction.

Results

Preexposure of U937 and Multiple Other Human Leukemia Cells to LAQ-824 Synergistically Increases Fludarabine-Induced Apoptosis

Analogous to earlier results with MS-275 and fludarabine in Jurkat cells (5), regimens combining the hydroxamic acid derivative pan-HDACI LAQ-824 and fludarabine were optimized in U937 myelomonocytic leukemia cells. Administered individually, 40 nmol/L LAQ-824 (40 h) and

0.4 μmol/L fludarabine (24 h) were only minimally toxic; however, when administered sequentially, apoptosis was very pronounced (e.g., ~80%; Fig. 1A). Time-course analysis revealed a marked increase in lethality between 8 and 16 h following addition of fludarabine to LAQ-824-pretreated cells (Fig. 1A). As with MS-275 (5), only additive interactions were observed with simultaneous administration (L_{24 h}→F_{24 h}: 35.4 ± 1.3%) or sequentially with fludarabine followed by LAQ-824 (fludarabine_{48 h}: 17.6 ± 0.9%; LAQ-824_{24 h}: 9.4 ± 0.2%; F_{24 h}→L_{24 h}: 37.2 ± 2.3%; data not shown). Clonogenic assays revealed that sequential exposure of U937 cells to LAQ-824 (24 h) followed by fludarabine dramatically reduced colony formation (Fig. 1A, right), indicating that LAQ-824/fludarabine interactions do not merely reflect acceleration of cell death. Sequential LAQ-824/fludarabine was active against diverse leukemia cells including HL-60 promyelocytic leukemia cells, Jurkat T human lymphoblastic leukemia cells, and K562 chronic myelogenous leukemia cells (Supplementary Fig. S1).⁴ Pronounced loss of mitochondrial membrane potential following sequential administration LAQ-824/fludarabine was observed in U937 cells (Supplementary Fig. S2A),⁴ accompanied by marked cytochrome *c*, apoptosis-inducing factor, and Smac cytoplasmic release (Supplementary Fig. S2B).⁴ These events were accompanied by caspase-9, -7, -3 and -8 and Bid activation and poly(ADP-ribose) polymerase degradation (Supplementary Fig. S2C).⁴

Early but Not Late ROS Generation Plays a Critical Functional Role in LAQ-824/Fludarabine-Induced Lethality

Although ROS generation has been implicated in the lethality of HDACIs alone (19, 22, 23) and fludarabine/MS-275 interactions (5), a detailed analysis of its role in HDACI/nucleoside analogue interactions has not been undertaken. Time-course studies in U937 cells exposed to LAQ-824/fludarabine (Fig. 1B) revealed a pronounced increase in ROS, reflected by the oxidation-sensitive dye 2',7'-dichlorodihydrofluorescein diacetate (20 μmol/L; left), 30 min after exposure to 40 nmol/L LAQ-824, which remained elevated for 2 to 4 h and returned to baseline by 6 to 8 h. Significantly, fludarabine administered alone or following 24 h preexposure to LAQ-824 (Fig. 1B, left) did not induce the generation of ROS. Similar effects were observed with another oxidation-sensitive dye, dihydroethidium (5 μmol/L; Fig. 1B, right).

To determine the functional significance of the initial ROS induction by LAQ-824, U937 cells were exposed sequentially to LAQ-824/fludarabine (L_{24 h}→F_{24 h}) in the presence of the ROS scavenger *N*-acetylcysteine (NAC; Fig. 1C). NAC was added either 2 h before LAQ-824 (+NAC 2 h) or 2 h before fludarabine (+NAC 22 h). Notably, NAC added before LAQ-824 (+NAC 2 h) completely

⁴ Supplementary material for this article is available at Molecular Cancer Therapeutics Online (<http://mct.aacrjournals.org/>).

blocked LAQ-824-induced early ROS generation (Fig. 1B, right) and markedly protected cells from LAQ-824/fludarabine lethality ($P < 0.01$; Fig. 1C). In marked contrast, addition of NAC shortly before fludarabine (+NAC 22 h)

had no effect on lethality ($P > 0.05$). Concordant results were obtained monitoring cleavage/activation of caspase-3 and -7 and poly(ADP-ribose) polymerase degradation (Fig. 1C) or in Jurkat cells exposed to LAQ-824/fludarabine

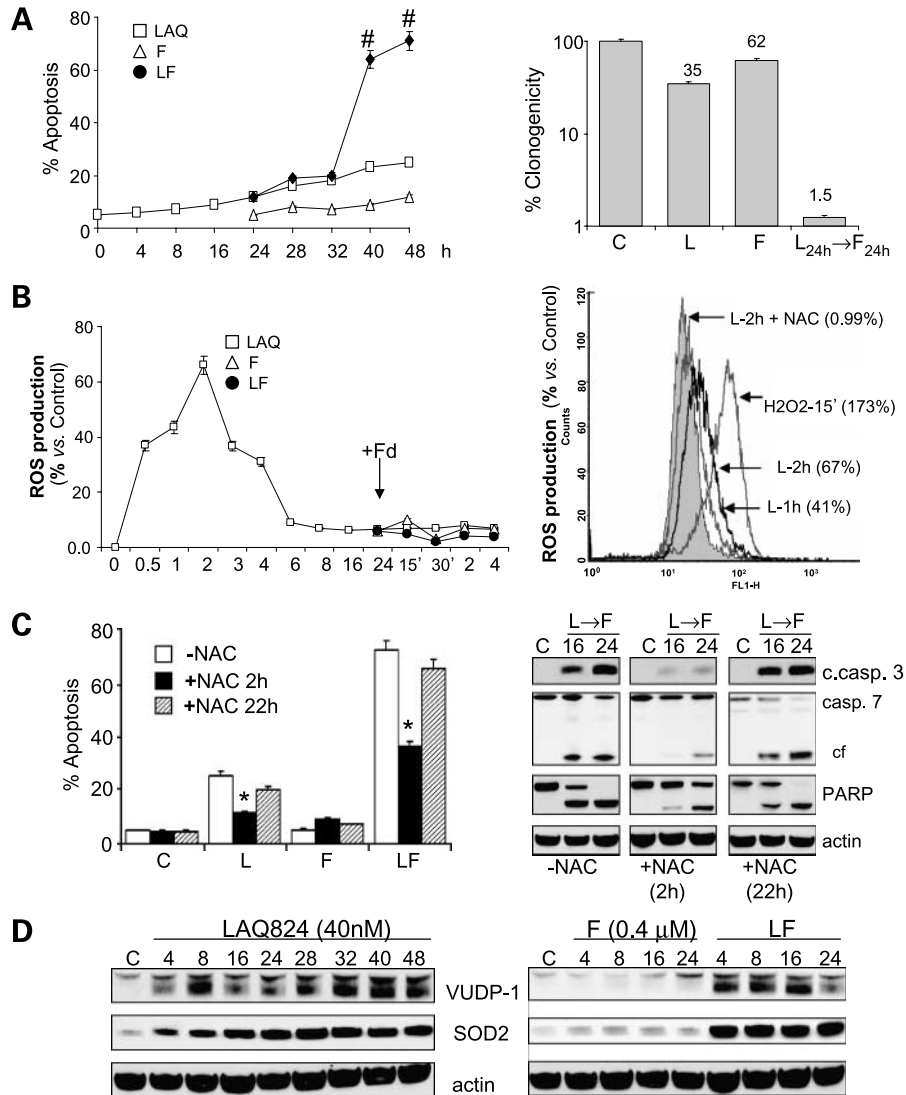


Figure 1. Preexposure of U937 cells to LAQ-824 synergistically increases fludarabine-induced apoptosis in an early ROS generation-dependent manner. **A**, left, time-course analysis of cell death induced by exposure of U937 cells to 40 nmol/L LAQ-824 (L) for 24 h, after which they were either left untreated or exposed to fludarabine (0.4 μ mol/L) without washing. Cells were collected at the indicated intervals and the extent of apoptosis was determined by Annexin V/PI analysis as described in Materials and Methods. #, $P < 0.001$, significantly greater than values from cells treated with either drug alone. Clonogenic assay analysis was done in cells sequentially exposed to LAQ-824 (48 h), fludarabine (24 h), or the two agents in combination (L_{24 h}→F_{24 h}). Colonies, consisting of groups of ≥ 50 cells, were scored after 12 days. Mean \pm SD of three separate experiments done in triplicate. **B**, U937 cells were exposed sequentially to LAQ-824/fludarabine for the indicated intervals, after which they were labeled with the oxidation-sensitive dyes 2',7'-dichlorodihydrofluorescein diacetate (20 μ mol/L; left) or dihydroethidium (5 μ mol/L; right) and analyzed by flow cytometry to determine the percentage of cells displaying an increase in ROS production relative to untreated controls. Mean \pm SE of three separate experiments. **C**, U937 cells were exposed sequentially to LAQ-824 (48 h), fludarabine (24 h), or the sequential combination (L_{24 h}→F_{24 h}) \pm the free radical scavenger NAC (15 mmol/L) administered either (a) 2 h before the administration of LAQ-824 (+NAC 2 h) or (b) after 22 h of treatment with LAQ-824 (2 h before the addition of fludarabine to LAQ-824-pretreated cells; +NAC 22 h). Cells were collected after 24 h exposure to fludarabine and analyzed by flow cytometry to determine the percentage of Annexin V/PI-positive cells. *, $P < 0.01$, significantly lower than cells exposed to LAQ-824 alone or sequentially to LAQ-824/fludarabine in the absence of NAC. **Right**, lysates from cells analyzed by flow cytometry were collected for Western blot analysis of proteins for the indicated intervals; cell lysates were prepared and 30 μ g protein was separated by SDS-PAGE, blotted, and probed with the indicated antibodies. c, caspase-3; cleaved caspase-3; cf, cleavage fragment. **D**, Western blot analysis of proteins from U937 cells exposed to LAQ-824 (40 nmol/L), fludarabine, or the sequential combination (L_{24 h}→F) for the indicated intervals; 30 μ g protein was separated by SDS-PAGE, blotted, and probed with the corresponding antibodies. Blots were subsequently stripped and reprobed with antibodies directed against actin to ensure equivalent loading and transfer. In all cases, representative results are shown; two additional experiments yielded similar results.

in the absence or presence of NAC (-2 h; Supplementary Fig. S3A).⁴ This suggests that early LAQ-824-mediated ROS induction plays an important functional role in LAQ-824/fludarabine lethality but argues strongly against the notion that LAQ-824 pretreatment simply increases fludarabine-mediated oxidative injury.

To gain insights into ROS regulation, Western blot analyses were done using U937 cells exposed sequentially to LAQ-824/fludarabine, and expression of proteins known to modulate ROS levels, including thioredoxin, thioredoxin reductase, VDRP1/TBP2, and (SOD1 and SOD2), were monitored (Fig. 1D; Supplementary Fig. S3B).⁴ No changes in thioredoxin, thioredoxin reductase, or SOD1 levels were detected under any experimental condition (Supplementary Fig. S3B).⁴ However, an early time-dependent increase in expression of Mn-SOD2 and VDRP1/TBP2 was observed in cells exposed to LAQ-824 ± fludarabine (Fig. 1D), consistent with previous reports showing up-regulation of these proteins by HDACi in other cell types (24–26).

Induced Mn-SOD2 Regulates LAQ-824-Mediated ROS Generation

To investigate the role of Mn-SOD2, U937 cells were sequentially exposed to LAQ-824/fludarabine in the presence or absence of the ROS scavenger and SOD2 mimetic Mn-TBAP. As with NAC (Fig. 1C), Mn-TBAP was added 2 h before LAQ-824 (+TBAP 2 h) or fludarabine (+TBAP 22 h). LAQ-824-induced ROS generation was markedly inhibited by Mn-TBAP (+TBAP 2 h; data not shown), which also strikingly diminished apoptosis (66.7 ± 4.5 versus 11.8 ± 3.5 , ±Mn-TBAP, respectively; Fig. 2A) and poly-(ADP-ribose) polymerase degradation (Fig. 2A, *bottom*). Notably, TBAP addition 2 h before fludarabine did not modify LAQ-824/fludarabine lethality (Fig. 2A). Additionally, U937 cells were transiently transfected with a cDNA coding for full-length Mn-SOD2 and exposed to LAQ-824/fludarabine (Fig. 2B). Enforced expression of Mn-SOD2 blocked LAQ-824-induced ROS (U937/EV: 63% versus U937/Mn-SOD2: 13%; Fig. 2B, *top*) and dramatically diminished apoptosis (Fig. 2B, *bottom*), arguing that early LAQ-824-induced ROS generation is critical for lethality. Notably, U937 cells stably transfected with full-length antisense Mn-SOD2 cDNA (U/SOD2-AS) displayed no detectable LAQ-824-induced Mn-SOD2 (Fig. 2C) and exhibited persistently increased ROS levels (data not shown) as well as increased sensitivity to LAQ-824 ± fludarabine (Fig. 2C, *right*; $P < 0.05$). Collectively, these findings suggest that early LAQ-824-mediated ROS generation plays a critical functional role in LAQ-824/fludarabine lethality and that Mn-SOD2 is a key ROS regulator.

HDACI-Mediated ROS Generation Induces DNA Damage

In view of evidence that HDACi induce DNA damage and perturb repair activity (27–30) and that ROS modulate DNA integrity (31, 32), the possibility arose that LAQ-824-induced ROS disrupted DNA and promoted fludarabine-mediated DNA damage. Levels of phosphorylated histone H2AX (γ -H2AX), an early markers of DNA damage (27), were therefore monitored by Western blot in U937 cells

exposed to LAQ-824 (40 nmol/L) for 2 or 24 h (Fig. 3A). LAQ-824 significantly increased γ -H2AX levels as early as 2 h after administration, which increased further by 24 h (Fig. 3A). Importantly, LAQ-824-mediated increases in γ -H2AX were abolished by coincubation with NAC or Mn-TBAP (Fig. 3A). Similar results were obtained in cells treated with MS-275 (2 μ mol/L), a potent ROS inducer (ref. 19; data not shown). As purine nucleoside analogues such as fludarabine inhibit both DNA synthesis and repair, thereby inducing accumulation of DNA strand breaks (reviewed in ref. 33), more detailed studies were done. LAQ-824 treatment triggered a clear increase in γ -H2AX levels, which persisted and increased slightly beyond 24 h (Fig. 3B). In contrast, fludarabine (0.4 μ mol/L) increased γ -H2AX levels at relatively late exposure intervals (24 h), increasing slightly thereafter. However, cells pretreated (24 h) with LAQ-824 displayed an accelerated and very pronounced increase in γ -H2AX between 8 and 16 h following fludarabine exposure (Fig. 3B). Importantly, addition of NAC (Fig. 3C) or Mn-TBAP (data not shown) 2 h before LAQ-824 (+NAC 2 h) dramatically reduced γ -H2AX levels in cells exposed to either LAQ-824 or LAQ-824/fludarabine. In agreement with evidence that fludarabine did not affect ROS (Fig. 1B), addition of NAC to fludarabine-treated cells (24 h) did not modify γ -H2AX expression, indicating that fludarabine-induced DNA damage represents a ROS-independent process at the fludarabine concentrations used here (0.4 μ mol/L). Consistent with cell death data (Fig. 1C), no differences in γ -H2AX levels were observed when NAC was added immediately before fludarabine to LAQ-824-preexposed cells (Fig. 3C, *bottom*). In agreement with γ -H2AX findings, analysis of either phospho-ATM, an established indicator of DNA damage, by both foci formation and Western blot (Fig. 3D), or comet DNA damage assays (single-cell gel electrophoresis; Supplementary Fig. S4A)⁴ yielded similar results. Specifically, treatment with fludarabine or LAQ-824 individually only modestly induced ATM phosphorylation or ATM foci (Fig. 3D), whereas both foci formation and phospho-ATM (Western blot) were substantially increased in cells sequentially exposed to LAQ-824/fludarabine ($L_{24\text{ h}} \rightarrow F_{8\text{ h}}$). Similarly, minimal comet formation occurred in cells exposed to fludarabine for 16 h, whereas DNA damage was apparent following LAQ-824 exposure (24 h; Supplementary Fig. S6A).⁴ However, sequential exposure to LAQ-824/fludarabine induced substantially wider and longer comet tails after addition of fludarabine to LAQ-824-pretreated cells ($L_{24\text{ h}} \rightarrow F_{16\text{ h}}$), consistent with changes in γ -H2AX and phospho-ATM formation (Fig. 3). These results provide evidence of a link between LAQ-824-mediated early ROS generation and LAQ-824/fludarabine-induced DNA damage.

To exclude the possibility that increased γ -H2AX levels in LAQ-824/fludarabine-treated cells represented secondary apoptotic effects, cells were treated with LAQ-824/fludarabine in the presence of the pan-caspase inhibitor BOC-fmk (Supplementary Fig. S4B).⁴ Although apoptosis was significantly reduced by BOC-fmk ($L_{24\text{ h}} \rightarrow F_{16\text{ h}}$: $67.4 \pm 4.5\%$

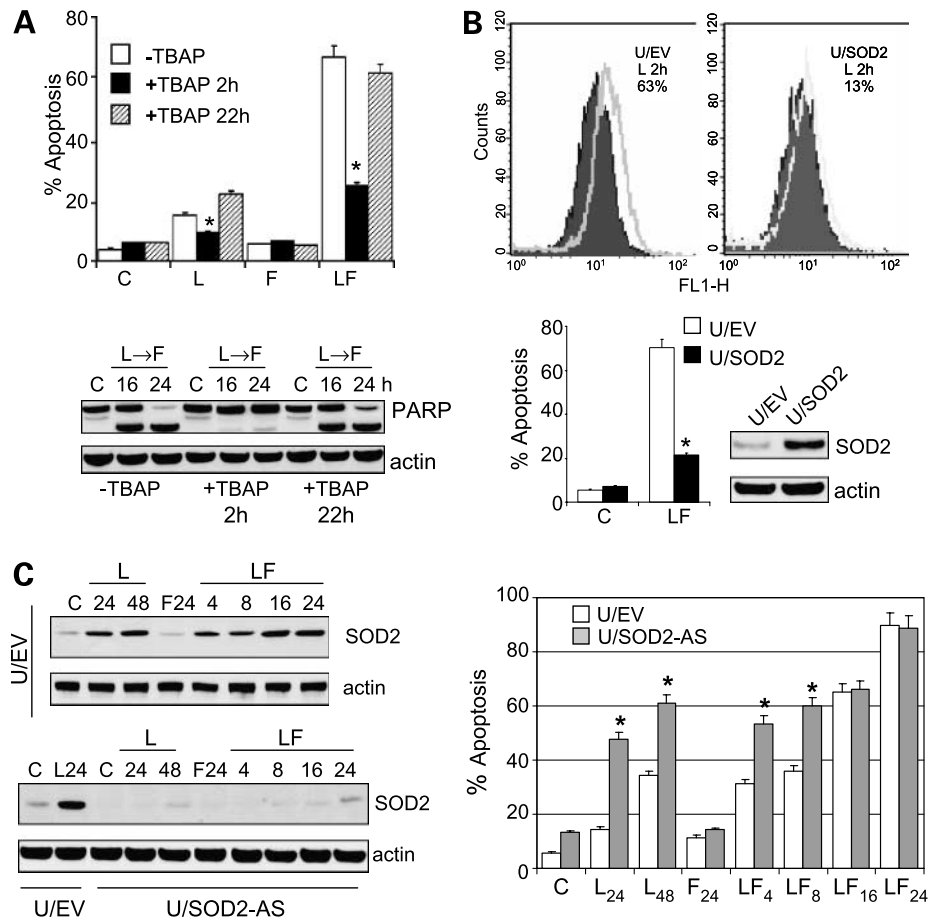


Figure 2. Role of LAQ-824-mediated Mn-SOD2 expression in LAQ-824/fludarabine-induced lethality. **A**, U937 cells were exposed sequentially to LAQ-824 (48 h), fludarabine (24 h), or the sequential combination ($L_{24\text{ h}} \rightarrow F_{24\text{ h}}$) in the presence or absence of the free radical scavenger Mn-TBAP (400 $\mu\text{mol/L}$) administered either (a) 2 h before the administration of LAQ-824 (+TBAP 2 h) or (b) after 22 h of treatment with LAQ-824 (2 h before the addition of fludarabine to LAQ-824-pretreated cells; +TBAP 22 h). Cells were collected after 24 h exposure to fludarabine and analyzed by flow cytometry to determine the percentage of Annexin V/PI-positive cells. *, $P < 0.01$, significantly lower than cells exposed sequentially to LAQ-824/fludarabine in the absence of Mn-TBAP. *Bottom*, Western blot analysis of U937 cells lysates prepared after sequential exposure to LAQ-824/fludarabine either in the absence or presence of Mn-TBAP as described in **A**. **B**, U937 cells transiently transfected with a full-length Mn-SOD2 cDNA were treated sequentially with LAQ-824/fludarabine as above, after which ROS production (*top*) and apoptosis (*bottom*) were determined by flow cytometry as described previously. *Inset*, Western blot showing Mn-SOD2 expression in U937 cells transiently transfected before treatment. **C**, U937 cells stably transfected with either empty pcDNA3.1 (U/EV) or with a Mn-SOD2 full-length cDNA oriented in the antisense direction were exposed to LAQ-824/fludarabine as above, after which they were analyzed by Western blot for expression of Mn-SOD2 (*left*) or for apoptosis by Annexin V/PI as described in Materials and Methods (*right*). *, $P < 0.01$, significantly greater than U937 cells transfected with the empty vector. **A** to **C**, lanes were loaded with 30 μg protein; blots were subsequently stripped and reprobbed with antibodies directed against actin to ensure equivalent loading and transfer. In all cases, representative results are shown; two additional experiments yielded similar results.

versus $L_{24\text{ h}} \rightarrow F_{16\text{ h}} + \text{BOC}$: $34.7 \pm 3.2\%$), $\gamma\text{-H2AX}$ expression remained largely unchanged, arguing that LAQ-824-mediated ROS induction and DNA damage represented a cause rather than a consequence of cell death.

Enhanced LAQ-824/Fludarabine Lethality Is Associated with LAQ-824-Mediated Down-regulation/Acetylation of DNA Repair Proteins and Disruption of DNA Repair

In view of evidence linking fludarabine DNA incorporation to lethality (13), the possibility that increased misincorporation of 2-fluoroadenine 9- β -D-arabinofuranoside-monophosphate into DNA might account for

enhanced DNA damage by the LAQ-824 regimen was investigated. LAQ-824 induced a progressive increase in the percentage of cells in $G_0\text{-}G_1$ accompanied by a decrease in S-phase cells ($G_0\text{-}G_1$ phase, C: 52%, LAQ-824_{24\text{ h}}}: 62.96%; LAQ-824_{32\text{ h}}}: 69.1%; S phase, C: 35.27%, LAQ-824_{24\text{ h}}}: 26.43%; LAQ-824_{32\text{ h}}}: 24.04%; Supplementary Fig. S5A).⁴ Consistent with these findings, LAQ-824 moderately reduced F-ara-A (DNA) incorporation compared with cells treated with fludarabine alone (ratio LAQ-824-fludarabine/fludarabine: 0.69 and 0.73 at the 6 and 16 h intervals, respectively; Supplementary Fig. S5B),⁴ suggesting enhanced apoptosis in cells exposed to the

LAQ-824/fludarabine regimen is unlikely to stem from potentiation of F-ara-A incorporation into DNA.

In view of evidence that HDACIs disrupt DNA repair (28, 30, 34), Western blot analysis of key components of the DNA repair machinery, including Ku70, Ku86, and Rad50, was done. Whereas Ku70 levels did not change following exposure to LAQ-824 (\pm fludarabine), expression of both Ku86 and Rad50 was significantly diminished (Fig. 4A, *left*). However, treatment with LAQ-824 \pm fludarabine increased Ku70 acetylation (Fig. 4A, *right*), a post-translational modification that modifies Ku70 activity (35). Analysis of DNA end-binding activity of both Ku70 and Ku86 in nuclear extracts of cells exposed to agents alone or in combination showed a dramatic decline in binding affinity of both proteins following LAQ-824 exposure ($P < 0.01$; Fig. 4C). Expression analysis of genes involved in DNA damage pathways revealed significant perturbations in several other repair-related genes, including *BRCA1*, *CHEK1*, *EXO1*, etc. (sample $L_{24\text{ h}} \rightarrow F_{8\text{ h}}$; Fig. 4C). Significantly, no differences were observed in

gene expression when the corresponding $L_{24\text{ h}} \rightarrow F_{8\text{ h}}$ profiles \pm TBAP (ROS scavenger) or $L_{24\text{ h}} \rightarrow F_{8\text{ h}}$ versus LAQ-824 $_{32\text{ h}}$ were compared with each other. This indicates that altered gene expression was independent of LAQ-824-mediated ROS generation and that gene expression changes reflected HDACI-mediated effects. Collectively, these findings suggest that LAQ-824 modifies the expression/function of multiple DNA repair proteins and raise the possibility that such actions contribute to potentiation of fludarabine-induced DNA damage and lethality.

Parallel studies were done with As_2O_3 (ATO), a compound that also induces ROS (ref. 36; Supplementary Fig. S6).⁴ Although ATO pretreatment increased fludarabine lethality and γ -H2AX formation, effects were only additive and more modest than those of LAQ-824, suggesting that although LAQ-824-induced ROS is critical to lethality, additional HDACI-mediated effects (e.g., perturbations in the DNA damage/repair machinery) are required for maximal activity.

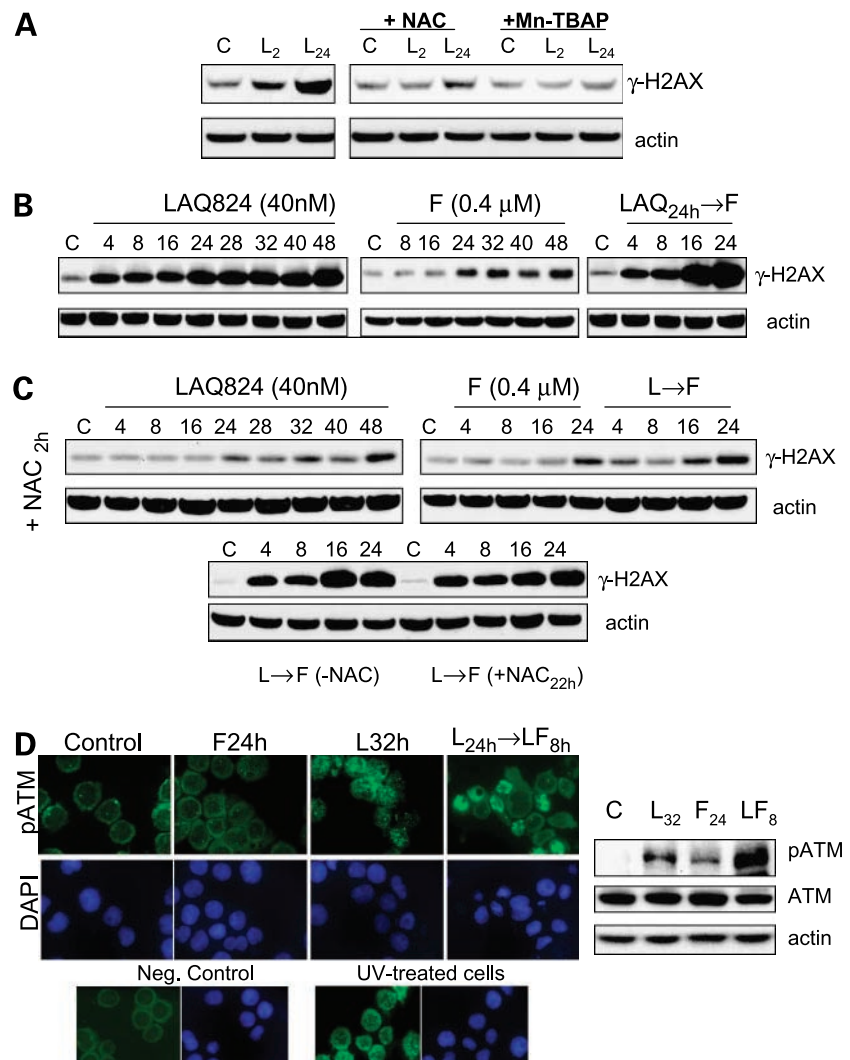


Figure 3. LAQ-824-mediated early oxidative injury promotes fludarabine-induced DNA damage. **A**, U937 cells were exposed to LAQ-824 (40 nmol/L) \pm the free radical scavengers NAC (15 mmol/L) or Mn-TBAP (400 μ mol/L) administered 2 h before addition of LAQ-824 for the indicated intervals, after which cell lysates were analyzed by Western blot to monitor expression of γ -H2AX as described in Materials and Methods. **B**, after exposure to LAQ-824 (40 nmol/L) and fludarabine (0.4 μ mol/L), either alone or in sequence for the indicated intervals, cell lysates were analyzed for γ -H2AX induction by Western blot as described in Materials and Methods. **C**, time-course analysis of γ -H2AX expression in U937 cells exposed to LAQ-824, fludarabine, or the sequential combination in the presence or absence of the free radical scavenger NAC (15 mmol/L). NAC was administered either 2 h before the addition of LAQ-824 (+NAC_{2 h}; *top*) or before addition of fludarabine to LAQ-824-pretreated cells (+NAC_{22 h}; *bottom*). **D**, U937 cells were treated with LAQ-824 (32 h), fludarabine (24 h), or with the combination $L_{24\text{ h}} \rightarrow F_{8\text{ h}}$, after which samples were prepared for both immunocytochemical analysis of phospho-ATM foci formation and Western blot analysis for total and phospho-ATM expression as described in Materials and Methods. **A to D**, lanes were loaded with 30 μ g protein; blots were subsequently stripped and reprobbed with antibodies directed against actin to ensure equivalent loading and transfer. In all cases, representative results are shown; two additional experiments yielded similar results.

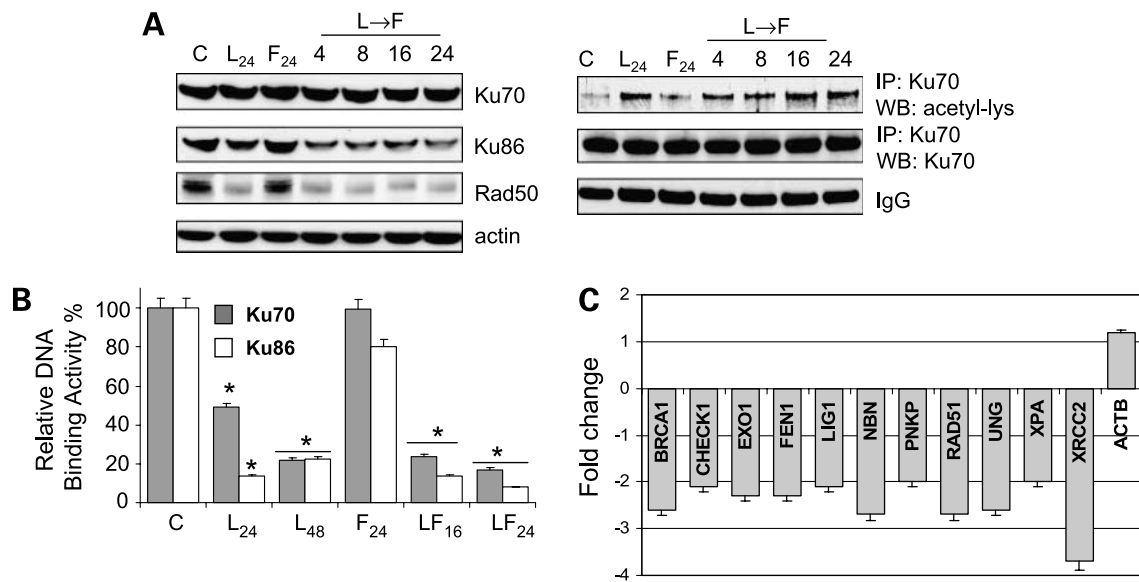


Figure 4. Exposure of cells to LAQ-824 perturbs DNA repair proteins. **A**, U937 cells were exposed to LAQ-824 (40 nmol/L), fludarabine (0.4 μ mol/L), or the combination in sequence (L_{24 h}→F) for the indicated intervals. *Left*, cell lysates were prepared and 30 μ g protein was separated by SDS-PAGE, blotted, and probed with the corresponding antibodies. Blots were subsequently stripped and reprobed with an antibody directed against actin to ensure equivalent loading and transfer. *Right*, analysis of Ku70 acetylation was determined by immunoprecipitating (IP) lysates with an anti-Ku70 antibody followed by immunoblotting (WB) with an anti-acetyl-lysine antibody as described in Materials and Methods. Each lane was loaded with 30 μ g protein; IgG controls confirm equivalent loading and transfer. Results of a representative study are shown; two additional experiments yielded similar results. **B**, analysis of DNA end-binding activity of Ku70 and Ku86 in nuclear extracts; cells were treated with LAQ-824 (40 nmol/L), fludarabine, or the combination in sequence (L_{24 h}→F) as described above for the indicated intervals, after which nuclear extracts were prepared and the DNA end-binding activity of Ku70/86 was quantitatively measured using a Ku70/86 DNA repair kit as described in Materials and Methods. Mean \pm SD of duplicate determinations done on three occasions; *, $P < 0.01$, significantly less than untreated control cells. **C**, analysis of genes involved in DNA damage/repair by RT² Profiler PCR microarray. U937 cells were exposed to L_{24 h}→F_{8 h}, after which RNA was extracted and analyzed by real-time reverse transcription-PCR as described in Materials and Methods. Fold change with respect to values for control RNA samples (untreated U937 cells) are shown. Gene description: *BRCA1*, breast cancer 1; *CHEK1*, CHK1 checkpoint homologue; *EXO1*, exonuclease 1; *FEN1*, flap structure-specific endonuclease 1; *LIG1*, ligase I, DNA, ATP-dependent; *NBN*, nibrin; *PNKP*, polynucleotide kinase 3'-phosphatase; *RAD51*, RAD51 homologue (RecA homologue, *Escherichia coli*; *Saccharomyces cerevisiae*); *UNG*, uracil-DNA glycosylase; *XPA*, xeroderma pigmentosum, complementation group A; *XRCC2*, X-ray repair complementing defective repair 2; and *ACTB*, β -actin (used as a control housekeeping gene). Mean \pm SE of three independent experiments.

LAQ-824/Fludarabine-Mediated Lethal Effects Involve Cytosolic Release of the Linker Histone H1.2 and Caspase-2 Activation

Recent studies reveal a chromatin-derived signal linking nuclear DNA damage to mitochondria via histone H1.2 release from the nucleus to the cytoplasm (37). Consequently, histone H1.2 expression was monitored in nuclear and cytoplasmic extracts obtained from cells exposed to LAQ-824/fludarabine (Fig. 5A). Exposure of U937 cells to LAQ-824 \pm fludarabine did not modify total histone H1.2 levels in nuclear extracts (Supplementary Fig. S5C).⁴ LAQ-824 moderately increased cytoplasmic histone H1.2, whereas fludarabine alone did not (Fig. 5A). However, sequential exposure of cells to LAQ-824 (24 h) followed by fludarabine (8 h) dramatically increased cytoplasmic histone H1.2 levels (Fig. 5A). Significantly, histone H1.2 release was minimal in cells treated sequentially with LAQ-824/fludarabine in the presence of TBAP (Fig. 5B) or NAC (data not shown) administered 2 h before LAQ-824. The functional role of released histone H1.2 was then assessed by monitoring lethality in cells stably expressing siRNA directed against histone H1.2 (U937/pS-H1.2 cells). Diminished histone H1.2 expression levels dramatically reduced LAQ-824/

fludarabine lethality (Fig. 5C; $P < 0.01$ versus controls). Moreover, histone H1.2 has been implicated in cytochrome *c* release, an event dependent on H1.2-induced Bak conformational activation and oligomerization (37, 38). Analysis of parental (data not shown) or transfected U937 cells with pSilencer control vector (U937/pS-C) revealed a marked increase in conformationally changed Bak following exposure to LAQ-824 alone (24–48 h) or in combination with fludarabine. However, these changes were dramatically reduced in cells depleted of histone H1.2 (U937/pS-H1.2; Fig. 5D). Finally, U937 cells stably transfected with a Bak-siRNA displayed significantly diminished lethality following sequential exposure to LAQ-824/fludarabine ($P < 0.01$; Fig. 5C).

In addition to histone H1.2, cleavage/activation of caspase-2, the only procaspase constitutively present in the nucleus (39), has been implicated in the apoptotic response to chromosomal breaks and DNA damage (39, 40). LAQ-824 administered alone or in combination induced a significant decline in the levels of procaspase-2, an event dramatically reduced by coincubation of cells with TBAP (Fig. 6A). Moreover, down-regulation of procaspase-2 by transiently transfecting U937 cells with siRNA (pSilencer caspase-2

sequences 13 and 18) significantly reduced ($\sim 30\%$; $P < 0.05$ versus scrambled sequence controls) LAQ-824/fludarabine lethality, consistent with DNA damage-mediated cell death (Fig. 6B). Reductions in procaspase-2 expression were documented by Western blot analysis (Fig. 6B, right). The dependence of caspase-2 activation on LAQ-824-mediated ROS was investigated further in U937 stably transfected with full-length antisense Mn-SOD2 cDNA. A time-course analysis revealed accelerated and more extensive activation of caspase-2 in U937/SOD2-AS cells compared with empty vector control cells following LAQ-824 and particularly LAQ-824/fludarabine treatment (Fig. 6C). These results indicate a functional link between cytoplasmic release of histone H1.2/caspase-2 activation and the ROS-dependent potentiation of fludarabine lethality by LAQ-824.

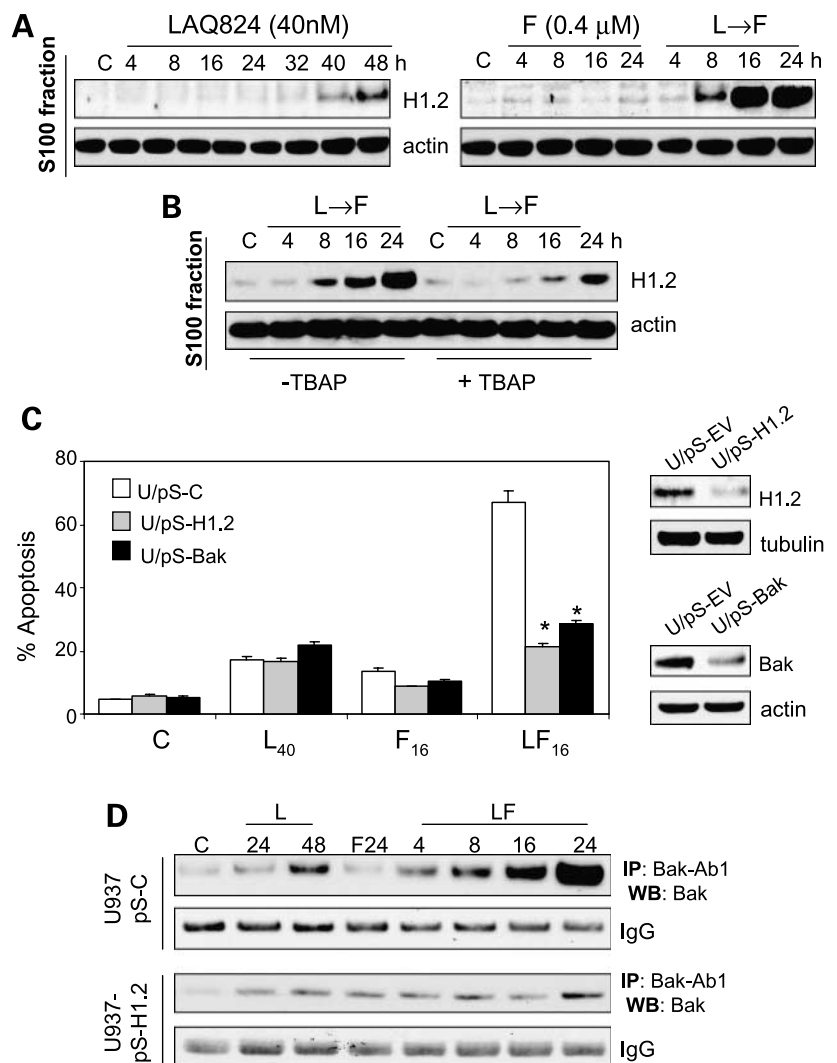
Discussion

The goal of this study was to gain further insights into mechanisms by which HDACi and, more specifically, a

pan-HDACi like LAQ-824, promote fludarabine lethality in human leukemia cells. The present findings suggest that this phenomenon involves multiple interrelated factors including early rather than late generation of ROS by LAQ-824, the resulting induction of LAQ-824-mediated DNA damage, and perturbations in the DNA repair machinery.

Recently, several studies have shown that HDACi enhance DNA damage induced by ionizing radiation and by certain cytotoxic agents, particularly DNA-damaging agents (27, 29, 41, 42), or can induce DNA damage by themselves (30). Although it has been proposed that HDACi-mediated sensitization to ionizing radiation may stem from inhibition of the DNA repair machinery (29, 34, 41), the mechanisms by which HDACi produce DNA damage are not well understood. In the case of intercalating agents, HDACi induce chromatin decondensation, which is more conducive to DNA-drug interactions (42). The present findings provide evidence that early HDACi-mediated ROS generation plays a critical role in sensitizing human leukemia cells to fludarabine lethality. Specifically, these

Figure 5. Cytosolic release of linker histone H1.2 and Bak activation contribute to LAQ-824/fludarabine-mediated lethality. **A**, U937 cells were treated with LAQ-824 (40 nmol/L), fludarabine (0.4 μ mol/L), or the sequential combination (L_{24 h}→F) as described above for the indicated intervals, pelleted, and lysed, and protein extracts were obtained from both nuclear and cytosolic S-100 fractions as described in Materials and Methods. Proteins (30 μ g) of S-100 fraction were separated by SDS-PAGE and probed with the corresponding antibodies directed against histone H1.2 or actin. Results of a representative study are shown; two additional experiments yielded similar results. **B**, U937 cells were exposed to (L_{24 h}→F) for the indicated intervals either in the absence or presence of the free radical scavenger and SOD2 mimetic Mn-TBAP (400 μ mol/L; added 2 h before exposure of cells to LAQ-824), after which the cytosolic S-100 fraction was extracted and 30 μ g protein was separated by SDS-PAGE and probed with the corresponding antibodies against histone H1.2 and actin. **C**, U937 cells stably expressing a scrambled sequence oligonucleotide siRNA (U/pS-C) or a sequence directed against either histone H1.2 or Bak (U/pS-H1.2 and U/pS-Bak, respectively) were exposed to LAQ-824 (40 h), fludarabine (16 h), or the combination in sequence (L_{24 h}→F_{16 h}), after which they were analyzed by flow cytometry to determine the percentage of Annexin V/PI-positive cells. *, $P < 0.01$, significantly lower than U/pS-C cells. **D**, analysis of Bak conformational change; U937/pS-C and U937/pS-H1.2 cells were treated as described in **A**, after which levels of conformationally changed Bak were determined by immunoprecipitating lysates with an anti-Bak-Ab1 antibody, which recognizes only the conformationally changed protein, followed by immunoblotting with an anti-Bak rabbit polyclonal antibody as described in Materials and Methods. Each lane was loaded with 30 μ g protein; IgG controls confirm equivalent loading and transfer. Results of a representative study are shown; two additional experiments yielded similar results. In all cases, mean \pm SD of three separate experiments done in triplicate.



results indicate that early HDACI-mediated ROS triggers DNA damage manifested by the appearance of γ -H2AX foci. The formation of γ -H2AX foci, which represent components of large DNA repair complexes (43), is one of

the earliest cellular responses to DNA damage (27). Inasmuch as the LAQ-824 concentrations used in this study were minimally toxic, the amount of DNA damage induced by this agent alone was only modestly lethal. However, it is

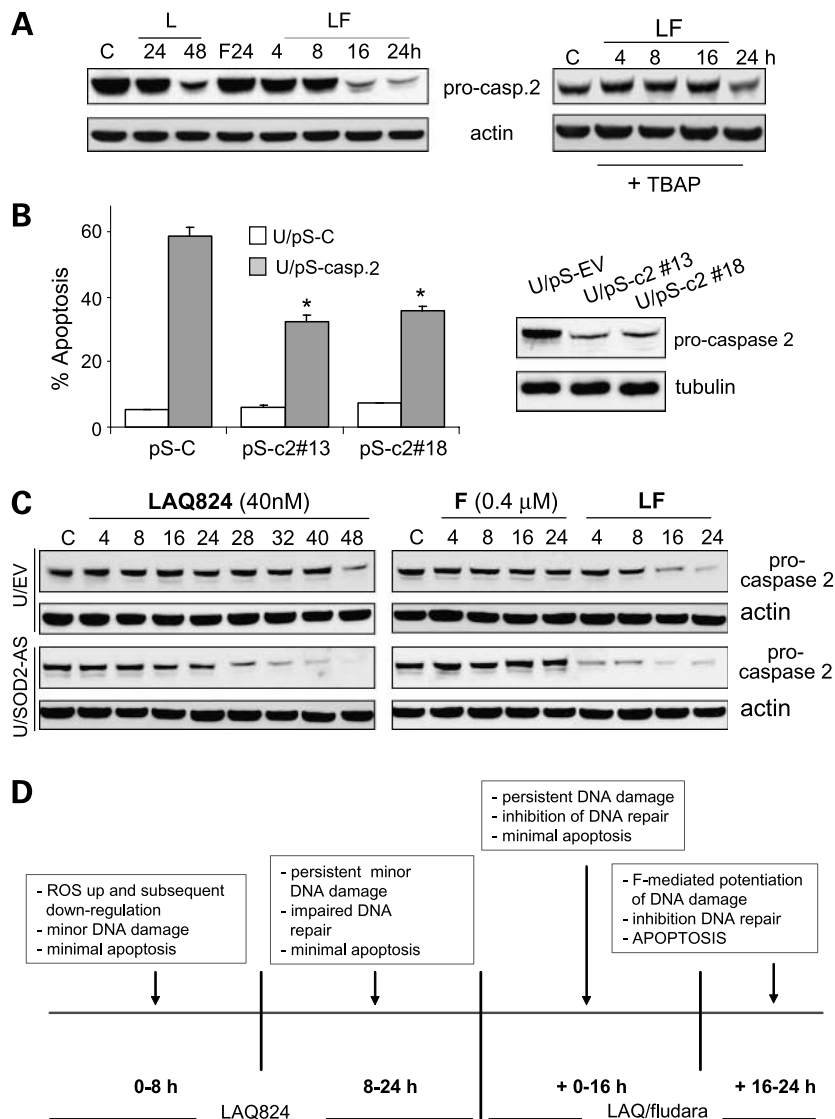


Figure 6. LAQ-824/fludarabine lethality involves caspase-2 activation. **A**, U937 cells were exposed to LAQ-824 (40 nmol/L), fludarabine, or the combination in sequence (L_{24 h}→F) for the indicated intervals either in the absence (*left*) or the presence (*right*) of the free radical scavenger and SOD2 mimetic Mn-TBAP (400 μ mol/L; added 2 h before LAQ-824), after which cell lysates were prepared. In each case, 30 μ g protein was separated by SDS-PAGE and probed with the corresponding antibodies against procaspase-2 and actin to document equivalent loading and transfer. **B**, U937 cells were transiently transfected with pSilencer vector encoding either a scrambled oligonucleotide siRNA (U/pS-C) or an oligonucleotide siRNA directed against procaspase-2 (U/pS-c2#13 and U/pS-c2#18); 24 h after transfection, cells were sequentially exposed to L_{24 h}→F_{16 h} as described above and analyzed by flow cytometry to determine the percentage of Annexin V/PI-positive cells. * $P < 0.05$, significantly lower than U/pS-C cells. **C**, both U937/EV and U937/SOD2-AS cells were treated as above and cell lysates were analyzed by Western blot for expression of procaspase-2 and, after stripping of blots, actin as described above. In all cases, results are representative and two additional experiments yielded similar results. **D**, model relating LAQ-824-mediated ROS production to LAQ-824/fludarabine lethality. According to this model, preexposure of cells to a minimally toxic concentration of LAQ-824 induces an early, marginally lethal increase in ROS, which, following induction of Mn-SOD2, is abolished approximately 8 h after addition of LAQ-824. During this interval, initial evidence of DNA damage (e.g., γ -H2AX formation) appears, although this is not by itself sufficient to trigger substantial activation of the apoptotic cascade. On addition of fludarabine (24 h after LAQ-824 administration), the initial ROS-mediated DNA damage persists, most likely due to LAQ-824-mediated inhibition of DNA repair. Subsequently, a dramatic increase in DNA damage occurs, which may reflect additional fludarabine-induced DNA breaks and/or further inhibition of repair. In this way, the addition of fludarabine produces levels of DNA damage that are incompatible with cell survival and triggers multiple proapoptotic signals including activation of nuclear caspase-2 and release of histone H1.2 into the cytoplasm. The latter event induces activation of Bak and culminates in pronounced mitochondrial injury and apoptosis.

likely that when DNA repair is compromised by genetic perturbations induced by HDACs and/or by disruption of repair by fludarabine (6, 11, 33), the extent of DNA damage exceeds a threshold level, and apoptosis ensues. Indeed, addition of fludarabine to LAQ-824-treated cells induced a striking increase in γ -H2AX expression and comet tail formation, a more direct indicator of DNA damage. Significantly, these events were largely abrogated by early coadministration of antioxidants or genetic interventions (enforced expression of Mn-SOD2), showing the critical role of early LAQ-824-mediated ROS production. Notably, although nucleoside analogue lethality in leukemic cells has been attributed to ROS generation (44), fludarabine by itself did not induce ROS generation in LAQ-824-pretreated cells, nor did addition of antioxidants immediately before fludarabine attenuate lethality, arguing that LAQ-824 does not act directly to enhance fludarabine-mediated oxidative injury.

ROS accumulation has been described in transformed cells exposed to structurally diverse HDACs, including vorinostat, trichostatin A, sodium butyrate, MS275, and LAQ-824 (19, 22, 23, 45, 46), and has been proposed as a mechanism underlying HDACi lethality. Notably, LAQ-824-mediated ROS accumulated within hours of drug exposure, whereas both Mn-SOD2 (an antioxidant protein) and VDRP1/TBP2 (a prooxidant protein) were induced early as reported previously with other HDACs (25, 26). Modulation of both VDRP1/TBP2 and thioredoxin expression has been implicated in HDACi lethality and invoked to explain differential responses to these agents by normal cells, which exhibit low ROS levels and are more resistant to HDACs, versus transformed cells, which display high ROS levels and are more susceptible to HDACs (47). In addition, transformed cells may be more susceptible to oxidative injury than their normal counterparts (48). In the present setting, despite VDRP1/TBP2 induction, early ROS increases were followed by an abrupt decline (within 6 h), most likely reflecting the rapid induction of Mn-SOD2. This notion is supported by evidence that transfectant cells initially displaying high Mn-SOD2 expression failed to generate ROS or DNA damage following LAQ-824 exposure.

The mechanism by which LAQ-824 disrupts the DNA repair machinery is likely to be multifactorial. Although LAQ-824-induced ROS generation resulted in DNA damage, reflected by increased phosphorylation/activation of both ATM and H2AX, the degree of damage, although only modestly lethal, was sustained. HDACs inhibit DNA repair by modulating the expression of important components of this machinery (29, 34). They also induce post-translational modifications of repair proteins such as inactivation of Ku70 by acetylation, which also diminishes its association with Ku80 as well as with Bax (35). In accord with these results, LAQ-824 induced down-regulation of Ku86, Rad50, and BRCA1, among other DNA repair proteins, induced Ku70 acetylation and diminished Ku70 and Ku86 DNA-binding activity, arguing that disruption of DNA repair very likely contributed to LAQ-824/fludarabine antileukemic synergism.

Recent evidence suggests a role for the linker histone H1.2 in DNA damage-induced apoptosis (37). DNA double-strand breaks induce cytoplasmic translocation of histone H1.2 where it promotes release of cytochrome *c* from mitochondria by activating the Bcl-2 family member Bak (37) and by forming a complex with Apaf-1, caspase-9, and cytochrome *c* (38). Notably, cytoplasmic localization of histone H1.2 and Bak activation/conformational change only occurred in association with enhanced DNA damage in cells sequentially exposed to LAQ-824 and fludarabine. The functional significance of these events was confirmed by evidence that knockdown of histone 1.2 or Bak significantly diminished the lethality of the LAQ-824 regimen. Importantly, release of histone H1.2 to the cytosol was markedly reduced in cells coincubated with the free radicals scavengers NAC or TBAP, further emphasizing the role of early LAQ-824-mediated ROS generation in both DNA damage and lethality.

In addition to histone H1.2 release, a role has been proposed for caspase-2 in DNA damage responses (49). Although procaspase-2 is present in several intracellular compartments, it is the only procaspase localizing constitutively to the nucleus (39) and provides a direct link between nuclear DNA damage responses and mitochondrial events (49, 50). Significantly, caspase-2 was markedly activated in response to increased DNA damage by the LAQ-824/fludarabine regimen, and caspase-2 knockdown by siRNA sharply reduced lethality. Nevertheless, this reduction was significantly less than that produced by H1.2 knockdown, which may reflect the fact that release of histone H1.2 acts, through Bak activation, directly on mitochondria and may have a more critical effect on apoptosis amplification. The findings that genetic ablation of Mn-SOD2 promoted, whereas coadministration of antioxidants diminished, procaspase-2 activation provide a link between HDACi-mediated ROS generation, increased fludarabine-mediated DNA damage, and activation of the mitochondrial apoptotic cascade.

Taken together, the preceding findings suggest a theoretical model proposing specific roles for HDACi-mediated ROS generation and perturbations in DNA damage/repair in antileukemic interactions with fludarabine (Fig. 6D). According to this model, preexposure to LAQ-824 induces an early and transient increase in ROS that is reversed by Mn-SOD2 induction at a relatively early interval. The early generation of ROS nevertheless leads to DNA damage, manifested by γ -H2AX formation, although the extent of damage is insufficient by itself to trigger a pronounced apoptotic response. However, initial ROS-induced DNA damage persists very possibly due to LAQ-824-mediated inhibition/down-regulation of DNA repair proteins through transcriptional and/or post-translational mechanisms (e.g., acetylation). Despite its persistence, the DNA damage is only modestly lethal. However, subsequent addition of fludarabine, either by inducing additional DNA damage (6, 13) and/or by further disrupting repair (11, 12), triggers a dramatic increase in DNA damage, the extent of which is now incompatible with cell survival. Irreversible

death signals are then triggered by activation of nuclear caspase-2, cytoplasmic release of histone H1.2, and Bak activation, culminating in pronounced mitochondrial injury and apoptosis. Whether interference with DNA repair processes will increase the mutagenicity of purine nucleoside analogues such as fludarabine (51) remains to be determined. In any case, this model may provide a clearer mechanistic basis for understanding the role of early HDACI-induced ROS generation and modulation of DNA repair processes in potentiating nucleoside analog-mediated DNA damage and lethality in leukemia.

Disclosure of Potential Conflicts of Interest

P. Atadja: Novartis Pharmaceuticals, employee. The other authors disclosed no potential conflicts of interest.

References

- Dokmanovic M, Clarke C, Marks PA. Histone deacetylase inhibitors: overview and perspectives. *Mol Cancer Res* 2007;5:981–9.
- Bolden JE, Peart MJ, Johnstone RW. Anticancer activities of histone deacetylase inhibitors. *Nat Rev Drug Discov* 2006;5:769–84.
- Rosato RR, Grant S. Histone deacetylase inhibitors: insights into mechanisms of lethality. *Expert Opin Ther Targets* 2005;9:809–24.
- Johnstone RW, Licht JD. Histone deacetylase inhibitors in cancer therapy: is transcription the primary target? *Cancer Cell* 2003;4:13–8.
- Maggio SC, Rosato RR, Kramer LB, et al. The histone deacetylase inhibitor MS-275 interacts synergistically with fludarabine to induce apoptosis in human leukemia cells. *Cancer Res* 2004;64:2590–600.
- Robak T, Korycka A, Kasznicki M, Wrzesien-Kus A, Smolewski P. Purine nucleoside analogues for the treatment of hematological malignancies: pharmacology and clinical applications. *Curr Cancer Drug Targets* 2005;5:421–44.
- Thomas MB, Koller C, Yang Y, et al. Comparison of fludarabine-containing salvage chemotherapy regimens for relapsed/refractory acute myelogenous leukemia. *Leukemia* 2003;17:990–3.
- Struck RF, Shortnacy AT, Kirk MC, et al. Identification of metabolites of 9- β -D-arabinofuranosyl-2-fluoroadenine, an antitumor and antiviral agent. *Biochem Pharmacol* 1982;31:1975–8.
- Brockman RW, Cheng YC, Schabel FM, Jr., Montgomery JA. Metabolism and chemotherapeutic activity of 9- β -D-arabinofuranosyl-2-fluoroadenine against murine leukemia L1210 and evidence for its phosphorylation by deoxycytidine kinase. *Cancer Res* 1980;40:3610–5.
- Huang P, Chubb S, Plunkett W. Termination of DNA synthesis by 9- β -D-arabinofuranosyl-2-fluoroadenine. A mechanism for cytotoxicity. *J Biol Chem* 1990;265:16617–25.
- Li L, Keating MJ, Plunkett W, Yang LY. Fludarabine-mediated repair inhibition of cisplatin-induced DNA lesions in human chronic myelogenous leukemia-blast crisis K562 cells: induction of synergistic cytotoxicity independent of reversal of apoptosis resistance. *Mol Pharmacol* 1997;52:798–806.
- Moufarij MA, Sampath D, Keating MJ, Plunkett W. Fludarabine increases oxaliplatin cytotoxicity in normal and chronic lymphocytic leukemia lymphocytes by suppressing interstrand DNA crosslink removal. *Blood* 2006;108:4187–93.
- Huang P, Plunkett W. Fludarabine- and gemcitabine-induced apoptosis: incorporation of analogs into DNA is a critical event. *Cancer Chemother Pharmacol* 1995;36:181–8.
- Backway KL, McCulloch EA, Chow S, Hedley DW. Relationships between the mitochondrial permeability transition and oxidative stress during ara-C toxicity. *Cancer Res* 1997;57:2446–51.
- D'Autreaux B, Toledano MB. ROS as signalling molecules: mechanisms that generate specificity in ROS homeostasis. *Nat Rev Mol Cell Biol* 2007;8:813–24.
- Rosato RR, Almenara JA, Cartee L, et al. The cyclin-dependent kinase inhibitor flavopiridol disrupts sodium butyrate-induced p21WAF1/CIP1 expression and maturation while reciprocally potentiating apoptosis in human leukemia cells. *Mol Cancer Ther* 2002;1:253–66.
- Almenara J, Rosato R, Grant S. Synergistic induction of mitochondrial damage and apoptosis in human leukemia cells by flavopiridol and the histone deacetylase inhibitor suberoylanilide hydroxamic acid (SAHA). *Leukemia* 2002;16:1331–43.
- Rosato RR, Wang Z, Gopalkrishnan RV, Fisher PB, Grant S. Evidence of a functional role for the cyclin-dependent kinase-inhibitor p21WAF1/CIP1/MDA6 in promoting differentiation and preventing mitochondrial dysfunction and apoptosis induced by sodium butyrate in human myelomonocytic leukemia cells (U937). *Int J Oncol* 2001;19:181–91.
- Rosato RR, Almenara JA, Grant S. The histone deacetylase inhibitor MS-275 promotes differentiation or apoptosis in human leukemia cells through a process regulated by generation of reactive oxygen species and induction of p21CIP1/WAF1. *Cancer Res* 2003;63:3637–45.
- Harvey S, Decker R, Dai Y, et al. Interactions between 2-fluoroadenine 9- β -D-arabinofuranoside and the kinase inhibitor UCN-01 in human leukemia and lymphoma cells. *Clin Cancer Res* 2001;7:320–30.
- Chou TC, Talalay P. Quantitative analysis of dose-effect relationships: the combined effects of multiple drugs or enzyme inhibitors. *Adv Enzyme Regul* 1984;22:27–55.
- Ruefli AA, Ausserlechner MJ, Bernhard D, et al. The histone deacetylase inhibitor and chemotherapeutic agent suberoylanilide hydroxamic acid (SAHA) induces a cell-death pathway characterized by cleavage of Bid and production of reactive oxygen species. *Proc Natl Acad Sci U S A* 2001;98:10833–8.
- Rosato RR, Maggio SC, Almenara JA, et al. The histone deacetylase inhibitor LAQ-824 induces human leukemia cell death through a process involving XIAP down-regulation, oxidative injury, and the acid sphingomyelinase-dependent generation of ceramide. *Mol Pharmacol* 2006;69:216–25.
- Guo Z, Boekhoudt GH, Boss JM. Role of the intronic enhancer in tumor necrosis factor-mediated induction of manganous superoxide dismutase. *J Biol Chem* 2003;278:23570–8.
- Dai Y, Rahmani M, Dent P, Grant S. Blockade of histone deacetylase inhibitor-induced RelA/p65 acetylation and NF- κ B activation potentiates apoptosis in leukemia cells through a process mediated by oxidative damage, XIAP downregulation, and c-Jun N-terminal kinase 1 activation. *Mol Cell Biol* 2005;25:5429–44.
- Butler LM, Zhou X, Xu WS, et al. The histone deacetylase inhibitor SAHA arrests cancer cell growth, up-regulates thioredoxin-binding protein-2, and down-regulates thioredoxin. *Proc Natl Acad Sci U S A* 2002;99:11700–5.
- Zhang Y, Adachi M, Zou H, et al. Histone deacetylase inhibitors enhance phosphorylation of histone H2AX after ionizing radiation. *Int J Radiat Oncol Biol Phys* 2006;65:859–66.
- Munshi A, Kurland JF, Nishikawa T, et al. Histone deacetylase inhibitors radiosensitize human melanoma cells by suppressing DNA repair activity. *Clin Cancer Res* 2005;11:4912–22.
- Munshi A, Tanaka T, Hobbs ML, et al. Vorinostat, a histone deacetylase inhibitor, enhances the response of human tumor cells to ionizing radiation through prolongation of γ -H2AX foci. *Mol Cancer Ther* 2006;5:1967–74.
- Gaymes TJ, Padua RA, Pla M, et al. Histone deacetylase inhibitors (HDI) cause DNA damage in leukemia cells: a mechanism for leukemia-specific HDI-dependent apoptosis? *Mol Cancer Res* 2006;4:563–73.
- Barzilai A, Yamamoto K. DNA damage responses to oxidative stress. *DNA Repair (Amst)* 2004;3:1109–15.
- Tanaka T, Halicka HD, Huang X, Traganos F, Darzynkiewicz Z. Constitutive histone H2AX phosphorylation and ATM activation, the reporters of DNA damage by endogenous oxidants. *Cell Cycle* 2006;5:1940–5.
- Robak T, Lech-Maranda E, Korycka A, Robak E. Purine nucleoside analogs as immunosuppressive and antineoplastic agents: mechanism of action and clinical activity. *Curr Med Chem* 2006;13:3165–89.
- Zhang Y, Carr T, Dimtchev A, et al. Attenuated DNA damage repair by trichostatin A through BRCA1 suppression. *Radiat Res* 2007;168:115–24.
- Chen CS, Wang YC, Yang HC, et al. Histone deacetylase inhibitors sensitize prostate cancer cells to agents that produce DNA double-strand breaks by targeting Ku70 acetylation. *Cancer Res* 2007;67:5318–27.
- Jing Y, Dai J, Chalmers-Redman RM, Tatton WG, Waxman S. Arsenic trioxide selectively induces acute promyelocytic leukemia cell apoptosis via a hydrogen peroxide-dependent pathway. *Blood* 1999;94:2102–11.

37. Konishi A, Shimizu S, Hirota J, et al. Involvement of histone H1.2 in apoptosis induced by DNA double-strand breaks. *Cell* 2003;114:673–88.
38. Ruiz-Vela A, Korsmeyer SJ. Proapoptotic histone H1.2 induces CASP-3 and -7 activation by forming a protein complex with CYT c, APAF-1 and CASP-9. *FEBS Lett* 2007;581:3422–8.
39. Zhivotovsky B, Samali A, Gahm A, Orrenius S. Caspases: their intracellular localization and translocation during apoptosis. *Cell Death Differ* 1999;6:644–51.
40. Lassus P, Opitz-Araya X, Lazebnik Y. Requirement for caspase-2 in stress-induced apoptosis before mitochondrial permeabilization. *Science* 2002;297:1352–4.
41. Cuneo KC, Fu A, Osusky K, et al. Histone deacetylase inhibitor NVP-LAQ824 sensitizes human nonsmall cell lung cancer to the cytotoxic effects of ionizing radiation. *Anticancer Drugs* 2007;18:793–800.
42. Marchion DC, Bicaku E, Daud AI, Sullivan DM, Munster PN. Valproic acid alters chromatin structure by regulation of chromatin modulation proteins. *Cancer Res* 2005;65:3815–22.
43. van den BM, Bree RT, Lowndes NF. The MRN complex: coordinating and mediating the response to broken chromosomes. *EMBO Rep* 2003;4:844–9.
44. Hedley DW, McCulloch EA. Generation of reactive oxygen intermediates after treatment of blasts of acute myeloblastic leukemia with cytosine arabinoside: role of bcl-2. *Leukemia* 1996;10:1143–9.
45. Louis M, Rosato RR, Brault L, et al. The histone deacetylase inhibitor sodium butyrate induces breast cancer cell apoptosis through diverse cytotoxic actions including glutathione depletion and oxidative stress. *Int J Oncol* 2004;25:1701–11.
46. Ungerstedt JS, Sowa Y, Xu WS, et al. Role of thioredoxin in the response of normal and transformed cells to histone deacetylase inhibitors. *Proc Natl Acad Sci U S A* 2005;102:673–8.
47. Marks PA. Thioredoxin in cancer—role of histone deacetylase inhibitors. *Semin Cancer Biol* 2006;16:436–43.
48. Trachootham D, Zhou Y, Zhang H, et al. Selective killing of oncogenically transformed cells through a ROS-mediated mechanism by β -phenylethyl isothiocyanate. *Cancer Cell* 2006;10:241–52.
49. Norbury CJ, Zhivotovsky B. DNA damage-induced apoptosis. *Oncogene* 2004;23:2797–808.
50. Troy CM, Shelanski ML. Caspase-2 redox. *Cell Death Differ* 2003;10:101–7.
51. Maddocks-Christianson K, Slager SL, Zent CS, et al. Risk factors for development of a second lymphoid malignancy in patients with chronic lymphocytic leukaemia. *Br J Haematol* 2007;139:398–404.